MODELING AND IDENTIFICATION OF RATE-INDEPENDENT HYSTERESIS USING A SEMILINEAR DUHEM MODEL [1]

JinHyoung Oh and Dennis S. Bernstein

Department of Aerospace Engineering,
The University of Michigan, Ann Arbor, MI 48109-2140

Abstract: In this paper we consider a semilinear Duhem model. The input-output map of the model is rate-independent, thus yielding persistent phase shift (that is, hysteresis) at arbitrarily low frequency. For the semilinear Duhem model we reparameterize the response in terms of the control input, and we provide sufficient conditions for convergence to a hysteresis map. A constrained least squares method is developed to identify the hysteresis map using the semilinear Duhem model.

Keywords: Hysteresis, Modelling, Nonlinearity, Identification

1. INTRODUCTION

Hysteresis is a widespread phenomenon in many engineering areas. Although there is no precise definition of hysteresis, we adopt the intuitive notion that hysteresis is effectively *DC phase shift*, that is, phase shift that persists as the frequency content of the input signal approaches DC. Consequently, hysteresis is an inherently nonlinear phenomenon since the phase shift of linear systems always approaches zero degrees as the input frequency decreases.

To illustrate this point of view, consider the mechanism shown in Figure 1. The equation of motion is given by

$$m\ddot{q}(t) + c\dot{q}(t) + kd_w\left(q(t) - r(t)\right) = 0, \quad (1)$$

where $d_w(z)$ is the deadzone function with width w. Because of the deadzone at the attachment point, there is a phase shift between $r(t)$ and $q(t)$. The presence of hysteresis is not obvious during dynamic operation, since the phase shift is a consequence of both the gap and the dynamics.

[1] This research was supported in part by the National Science Foundation under grant ECS–0225799.

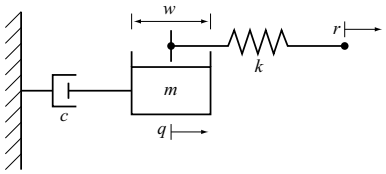

Fig. 1. Mass-dashpot-spring system with deadzone.

However, Figure 2 reveals that the phase shift persists near DC, that is, at asymptotically low frequency.

Alternatively, consider the relationship between the magnetic field $H(t)$ and the magnetic flux $B(t)$ of ferromagnetically soft materials of the isoperm type (Coleman and Hodgdon, 1986)

$$\dot{B}(t) = \alpha|\dot{H}(t)|[bH(t) - B(t)] + a\dot{H}(t). \quad (2)$$

Figure 3 shows the relationship between $H(t)$ and $B(t)$. The presence of phase shift for low frequency inputs indicates that this system is hysteretic.

Although the examples discussed above are both hysteretic, the response of the mass-spring system depends on the input frequency, or more generally, is affected by the time dependence of the input.

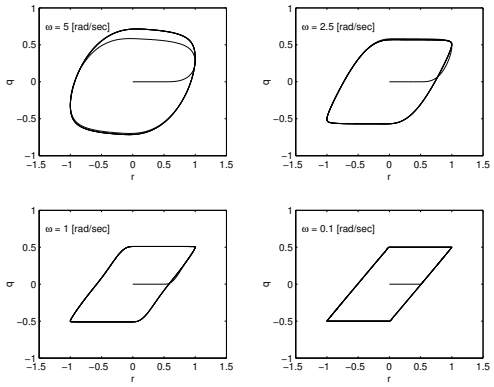

Fig. 2. Input-output map for the mass-dashpot-spring system with deadzone.

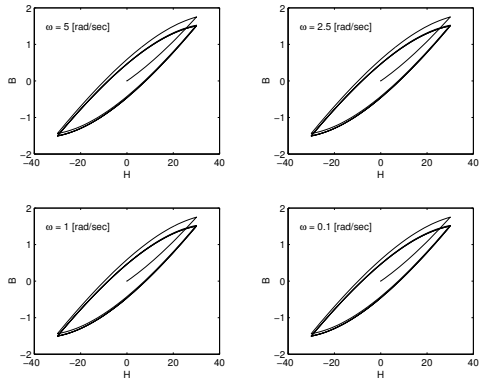

Fig. 3. Input-output map for the model of ferromagnetically soft materials of the isoperm type.

However, the ferromagnetic material model has the same input-output response for all frequencies and types of input.

One of the most successful hysteresis models is the Preisach model(Macki *et al.*, 1993, and references therein). Preisach models are frequency independent and thus they are inherently kinematic. However, Preisach models are computationally demanding, requiring gridding of the plane.

In contrast, the examples discussed above are finite dimensional, and thus they suggest alternatives to the Preisach model. In fact, both of these examples illustrate hysteresis models that have been studied in the literature. In particular, the mass-spring example is suggested in Kransnosel'skii and Pokrovskii (1980), p. 93, as an approximation to a hysteron model, while the ferromagnetic material model is a Duhem model, a class of hysteresis models extensively studied in Chua and Bass (1972).

The purpose of this paper is to extend the existing analysis of Duhem models in order to understand their properties for modeling and identification.

2. GENERALIZED DUHEM MODEL

Consider the single input-single output *generalized Duhem model* given by

$$\dot{x}(t) = f(x(t), u(t))g(\dot{u}(t)), \tag{3}$$
$$y(t) = h(x(t), u(t)), \quad x(0) = x_0,\ t \geq 0, \tag{4}$$

where $x \in \mathbb{R}^n$, $y \in \mathbb{R}$, $u \in \mathbb{R}$, $f : \mathbb{R}^n \times \mathbb{R} \to \mathbb{R}^{n\times r}$, and $g : \mathbb{R} \to \mathbb{R}^r$. We assume that the solution to (3) exists and is unique on all finite intervals. The following definition will be useful.

Definition 1. The generalized Duhem model (3), (4) is *time-scale invariant* if, for all $x(t)$ and $u(t)$ satisfying (3), all initial conditions x_0, and all $\alpha > 0$, it follows that $x_\alpha(t) \triangleq x(\alpha t)$ and $u_\alpha(t) \triangleq u(\alpha t)$ also satisfy (3).

The following definition is needed to characterize time-scale invariant generalized Duhem models.

Definition 2. The function g is *positively homogeneous* if $g(\alpha v) = \alpha g(v)$ for all $\alpha \geq 0$ and $v \in \mathbb{R}$.

The following result generalizes Property 9 of Chua and Bass (1972).

Proposition 1. Assume that g is positively homogeneous. Then the generalized Duhem model (3), (4) is time-scale invariant.

The time-scale invariant generalized Duhem model has several alternative representations. The following lemma is needed for further discussion.

Lemma 1. Assume g is positively homogeneous. Then there exist $h_+ \in \mathbb{R}^r$ and $h_- \in \mathbb{R}^r$ such that

$$g(v) = \begin{cases} vh_+, & v \geq 0, \\ vh_-, & v < 0. \end{cases} \tag{5}$$

Assume g is positively homogeneous. Then (3) and (4) can be rewritten as

$$\dot{x}(t) = \begin{cases} f_+\left(x(t), u(t)\right)\dot{u}(t), & \dot{u}(t) \geq 0, \\ f_-\left(x(t), u(t)\right)\dot{u}(t), & \dot{u}(t) < 0, \end{cases} \tag{6}$$
$$y(t) = h(x(t), u(t)),\ x(0) = x_0,\ t \geq 0, \tag{7}$$

where $f_+(x(t), u(t)) \triangleq f(x(t), u(t))h_+$ and $f_-(x(t), u(t)) \triangleq f(x(t), u(t))h_-$. Note that (6) can be viewed as a switching system with respect to the sign of $\dot{u}(t)$. Next define $\dot{u}_+(t) \triangleq \max\{0, \dot{u}(t)\}$, and $\dot{u}_-(t) \triangleq \min\{0, \dot{u}(t)\}$. Then (6) can be written as

$$\dot{x}(t) = [\dot{u}_+(t)I_n\ \dot{u}_-(t)I_n] \begin{bmatrix} f_+(x(t), u(t)) \\ f_-(x(t), u(t)) \end{bmatrix}, \tag{8}$$
$$y(t) = h(x(t), u(t)), \quad x(0) = x_0,\ t \geq 0. \tag{9}$$

which is the *classical Duhem model* (Macki *et al.*, 1993).

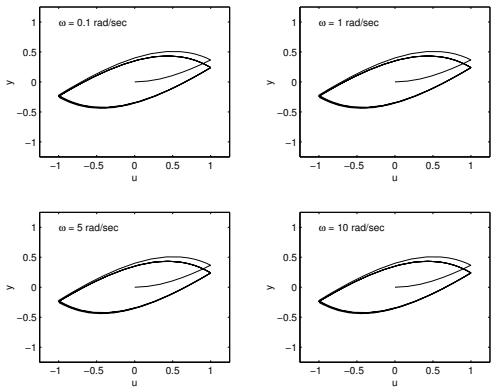

Fig. 4. Input-output maps of Example 1 with $g(\dot{u}) = |\dot{u}|$ and $u(t) = \sin t$.

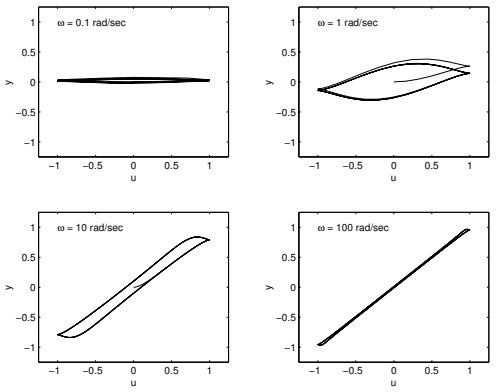

Fig. 5. Input-output maps of Example 1 with $g(\dot{u}) = \dot{u}^2$ and $u(t) = \sin t$.

Example 1. Consider the generalized Duhem model

$$\dot{x}(t) = (-x(t) + u(t))g(\dot{u}(t)), \tag{10}$$
$$y(t) = x(t), \quad x(0) = 0,\, t \geq 0,. \tag{11}$$

First, let $g(\dot{u}) = |\dot{u}|$. Since $|\dot{u}|$ is positively homogeneous, Proposition 1 implies that (10), (11) is time-scale invariant and the input-output maps of the model with different input frequencies are identical as shown in Figure 4. Next let $g(\dot{u}) = \dot{u}^2$, which is not positively homogeneous. Figure 5 shows that the input-output map of (10) and (11) depends on input frequency.

3. REPARAMETERIZATION OF THE TIME-SCALE INVARIANT GENERALIZED DUHEM MODEL

Consider the time-scale invariant generalized Duhem model (6), (7), where $u(t)$ is piecewise monotonic. Suppose $\dot{u}(t) \neq 0$. Then dividing both sides of (6) by $\dot{u}(t)$ yields

$$\frac{\mathrm{d}x(t)}{\mathrm{d}u(t)} = \begin{cases} f_+(x(t), u(t)), & \dot{u}(t) > 0, \\ f_-(x(t), u(t)), & \dot{u}(t) < 0. \end{cases} \tag{12}$$

Now suppose $\dot{u}(t) = 0$. Then (6) becomes $\dot{x}(t) = 0$ and thus $x(t)$ is constant. Therefore, the time-scale invariant generalized Duhem model (6), (7) can be reparameterized with u considered as the independent variable. Let $\hat{x}(u)$ and $\hat{y}(u)$ be the reparameterized variables of (6) and (7) such that $\hat{x}(u) \triangleq x(u(t))$ and $\hat{y}(u) \triangleq y(u(t))$. Then the reparameterized time-scale invariant generalized Duhem model becomes

$$\frac{\mathrm{d}\hat{x}(u)}{\mathrm{d}u} = \begin{cases} f_+(\hat{x}(u), u), & \text{if } u \text{ increases}, \\ f_-(\hat{x}(u), u), & \text{if } u \text{ decreases}, \end{cases} \tag{13}$$
$$\hat{y}(u) = h(\hat{x}(u), u), \quad \hat{x}(u_0) = x_0, \tag{14}$$

where $u_0 = u(0)$. Note that (13) and (14) can be viewed as a time-varying dynamical system with nonmonotonic time.

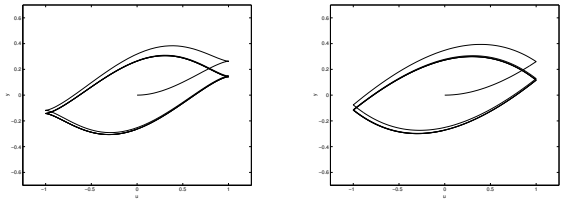

(a) (b)

Fig. 6. Input-output maps of Example 2 with $g(\dot{u}) = \dot{u}^2$ under (a) sinusoidal input, and (b) triangle input.

Example 2. Reconsider Example 1 with two different inputs, namely, sinusoidal and triangle inputs with same period and amplitude. When $g(\dot{u}) = |\dot{u}|$, the input-output maps under different inputs are identical. This shows that the input-output map is not affected by the time dependence of u. However, when $g(\dot{u}) = \dot{u}^2$, the input-output maps under different inputs are different as shown in Figure 6.

4. SEMILINEAR DUHEM MODEL

As a specialization of (8) and (9), in this section we consider the *semilinear Duhem model*

$$\dot{x}(t) = [\dot{u}_+(t) I_n \; \dot{u}_-(t) I_n] \times \left(\begin{bmatrix} A_+ \\ A_- \end{bmatrix} x(t) + \begin{bmatrix} B_+ \\ B_- \end{bmatrix} u(t) + \begin{bmatrix} E_+ \\ E_- \end{bmatrix} \right), \tag{15}$$
$$y(t) = Cx(t) + Du(t), \quad x(0) = x_0,\, t \geq 0, \tag{16}$$

where $A_+ \in \mathbb{R}^{n \times n}$, $A_- \in \mathbb{R}^{n \times n}$, $B_+ \in \mathbb{R}^n$, $B_- \in \mathbb{R}^n$, $E_+ \in \mathbb{R}^n$, $E_- \in \mathbb{R}^n$, $C \in \mathbb{R}^{1 \times n}$, and $D \in \mathbb{R}$. Note that (15), (16) are a time-scale invariant generalized Duhem model of the form (8), (9) with $f_+(x(t), u(t)) = A_+ x(t) + B_+ u(t) + E_+$, $f_-(x(t), u(t)) = A_- x(t) + B_- u(t) + E_-$, and $h(x(t), u(t)) = Cx(t) + Du(t)$. We exclude pathological inputs by assuming that $u(t)$ is piecewise monotonic. Reparameterizing (15) and (16) in terms of u yields

$$\frac{\mathrm{d}\hat{x}(u)}{\mathrm{d}u} = \begin{cases} A_+ \hat{x}(u) + B_+ u + E_+, \text{ if } u \uparrow, \\ A_- \hat{x}(u) + B_- u + E_-, \text{ if } u \downarrow, \end{cases} \tag{17}$$

$$\hat{y}(u) = C\hat{x}(u) + Du, \quad \hat{x}(u_0) = x_0, \tag{18}$$

where $u_0 = u(0)$. For the following lemma, A^{D} denote the Drazin generalized inverse of A and let $\operatorname{ind} A$ denote the index number of A (p. 122, Campbell and C. D. Meyer, 1979).

Lemma 2. Let $r_+ = \operatorname{ind} A_+$ and $r_- = \operatorname{ind} A_-$. Then the forward-time ramp response of (17) is given by $\hat{x}(u) = e^{A_+(u-u_0)}x_0 + \mathcal{X}_+(u,u_0) + \mathcal{Y}_+(u-u_0) - \mathcal{Z}_+(u,u_0)$, $u \geq u_0$, and the backward-time ramp response of (17) is given by $\hat{x}(u) = e^{A_-(u-u_0)}x_0 + \mathcal{X}_-(u,u_0) + \mathcal{Y}_-(u-u_0) - \mathcal{Z}_-(u,u_0)$, $u \leq u_0$, where

$$\mathcal{X}_+(u,u_0) \triangleq \left(I - A_+A_+^{\mathrm{D}}\right)\sum_{k=1}^{r_+}\frac{u+ku_0}{(k+1)!}(u-u_0)^k A_+^{k-1}B_+,$$

$$\mathcal{X}_-(u,u_0) \triangleq \left(I - A_-A_-^{\mathrm{D}}\right)\sum_{k=1}^{r_-}\frac{u+ku_0}{(k+1)!}(u-u_0)^k A_-^{k-1}B_-$$

$$\mathcal{Y}_+(u) \triangleq \left(I - A_+A_+^{\mathrm{D}}\right)\sum_{k=1}^{r_+}\frac{1}{k!}u^k A_+^{k-1}E_+,$$

$$\mathcal{Y}_-(u) \triangleq \left(I - A_-A_-^{\mathrm{D}}\right)\sum_{k=1}^{r_-}\frac{1}{k!}u^k A_-^{k-1}E_-,$$

$$\mathcal{Z}_+(u,u_0) \triangleq A_+^{\mathrm{D}}(uI - u_0e^{A_+(u-u_0)})B_+ + A_+^{2\mathrm{D}}\times (I - e^{A_+(u-u_0)})B_+ + A_+^{\mathrm{D}}(I - e^{A_+(u-u_0)})E_+,$$

$$\mathcal{Z}_-(u,u_0) \triangleq A_-^{\mathrm{D}}(uI - u_0e^{A_-(u-u_0)})B_- + A_-^{2\mathrm{D}}\times (I - e^{A_-(u-u_0)})B_- + A_-^{\mathrm{D}}(I - e^{A_-(u-u_0)})E_-,$$

Let $\rho(A)$ denote the spectral radius of $A \in \mathbb{R}^{n\times n}$. We now state the main result on the existence of hysteretic maps of the semilinear Duhem model.

Theorem 1. Let $u(t)$ and $y(t)$ satisfy the semilinear Duhem model (15), (16). Suppose $u(t)$ is piecewise monotonic and periodic with period T and has exactly one local maximum $u_{\max}$ in $[0,T)$ and exactly one local minimum $u_{\min}$ in $[0,T)$. Furthermore, let $\beta \triangleq u_{\max} - u_{\min}$ and assume that $\rho\left(e^{\beta A_+}e^{-\beta A_-}\right) < 1$. Then the input-output map of $u(t)$ and $y(t)$ converges to the closed curve in $\mathbb{R}^2$ given for $u \in [u_{\min}, u_{\max}]$ by

$$\begin{aligned}\hat{y}_+(u) &= Ce^{A_+(u-u_{\min})}\hat{x}_+ + C\mathcal{X}_+(u,u_{\min}) \\ &\quad + C\mathcal{Y}_+(u-u_{\min}) - C\mathcal{Z}_+(u,u_{\min}) + Du,\\ \hat{y}_-(u) &= Ce^{A_-(u-u_{\max})}\hat{x}_- + C\mathcal{X}_-(u,u_{\max}) \\ &\quad + C\mathcal{Y}_-(u-u_{\max}) - C\mathcal{Z}_-(u,u_{\max}) + Du,\end{aligned}$$

where

$$\begin{aligned}\hat{x}_+ &\triangleq \left(I - e^{-\beta A_-}e^{\beta A_+}\right)^{-1}\left(e^{-\beta A_-}\mathcal{W}_+ + \mathcal{W}_-\right),\\ \hat{x}_- &\triangleq \left(I - e^{\beta A_+}e^{-\beta A_-}\right)^{-1}\left(e^{\beta A_+}\mathcal{W}_- + \mathcal{W}_+\right),\\ \mathcal{W}_+ &\triangleq \mathcal{X}_+(u_{\max},u_{\min}) + \mathcal{Y}_+(\beta) - \mathcal{Z}_+(u_{\max},u_{\min}),\\ \mathcal{W}_- &\triangleq \mathcal{X}_-(u_{\min},u_{\max}) + \mathcal{Y}_-(-\beta) - \mathcal{Z}_+(u_{\max},u_{\min}).\end{aligned}$$

As a special case of (15), (16), consider the semilinear Duhem model

$$\dot{x}(t) = \begin{bmatrix}\dot{u}_+(t)I & \dot{u}_-(t)I\end{bmatrix} \times \left(\begin{bmatrix}h_+A\\ h_-A\end{bmatrix}x(t) + \begin{bmatrix}h_+B\\ h_-B\end{bmatrix}u(t) + \begin{bmatrix}h_+E\\ h_-E\end{bmatrix}\right), \tag{19}$$

$$y(t) = Cx(t) + Du(t), \quad x(0) = x_0,\ t \geq 0, \tag{20}$$

where $A \in \mathbb{R}^{n\times n}$, $B \in \mathbb{R}^n$, $E \in \mathbb{R}^n$, $h_+ \in \mathbb{R}$, $h_- \in \mathbb{R}$, $C \in \mathbb{R}^{1\times n}$, and $D \in \mathbb{R}$. The following result is the specialization of Theorem 1 to (19), (20).

Corollary 1. Let $u(t)$ and $y(t)$ satisfy the semilinear Duhem model (19), (20). Suppose A is asymptotically stable, and $u(t)$ is piecewise monotonic and periodic with period T and has exactly one local maximum $u_{\max}$ in $[0,T)$ and exactly one local minimum $u_{\min}$ in $[0,T)$. Furthermore, assume $h_- < h_+$. Then the input-output map of $u(t)$ and $y(t)$ converges to the closed curve in $\mathbb{R}^2$ given for $u \in [u_{\min}, u_{\max}]$ by

$$\begin{aligned}\hat{y}_+(u) &= Ce^{h_+A(u-u_{\min})}\hat{x}_+ + C\mathcal{V}_+(u) + Du,\\ \hat{y}_-(u) &= Ce^{h_-A(u-u_{\max})}\hat{x}_- + C\mathcal{V}_-(u) + Du,\end{aligned}$$

where

$$\hat{x}_+ \triangleq (I - e^{\beta(h_+-h_-)A})^{-1}(e^{-\beta h_-A}\mathcal{V}_+(u_{\max}) + \mathcal{V}_-(u_{\min})),$$

$$\hat{x}_- \triangleq (I - e^{\beta(h_+-h_-)A})^{-1}(e^{\beta h_+A}\mathcal{V}_-(u_{\min}) + \mathcal{V}_+(u_{\max})),$$

$$\mathcal{V}_+(u) \triangleq A^{-1}(uI - u_{\min}e^{h_+A(u-u_{\min})}B + h_+^{-1}A^{-2}\times (I - e^{h_+A(u-u_{\min})})B - A^{-1}(I - e^{h_+A(u-u_{\min})})E,$$

$$\mathcal{V}_-(u) \triangleq A^{-1}(uI - u_{\max}e^{h_-A(u-u_{\max})}B + h_-^{-1}A^{-2}\times (I - e^{h_-A(u-u_{\max})})B - A^{-1}(I - e^{h_-A(u-u_{\max})})E,$$

Example 3. Consider the semilinear Duhem model (19), (20) with

$$A = \begin{bmatrix}-1 & 4\\ -4 & -1\end{bmatrix},\ B = \begin{bmatrix}0\\ 1\end{bmatrix},\ C = \begin{bmatrix}0 & 1\end{bmatrix},$$
$$x_0 = \begin{bmatrix}0.15 & 0.15\end{bmatrix}^{\mathrm{T}}.$$

Suppose $u(t) = \sin t$, $t \geq 0$ and let $h_+ = 1$ and $h_- = -1$. Then since A is asymptotically stable and $h_- < h_+$, Corollary 1 implies that the input-output map of $u(t)$ and $y(t)$ converges to a closed curve as $t \to \infty$. Indeed, $\rho(e^{2h_+A}e^{-2h_-A}) = 0.0183 < 1$, and the closed curve is shown in Figure 7a. Now let $h_+ = 1$ and $h_- = 1.1$. Then $h_- > h_+$ and the input-output map of $u(t)$ and $y(t)$ does not converge, as shown in Figure 7b. In this case, $\rho(e^{2h_+A}e^{-2h_-A}) = 1.2214 > 1$.

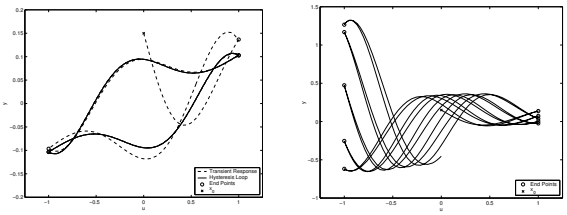

(a) (b)

Fig. 7. Input-output maps of Example 3 with $h_+ = 1$ and (a) $h_- = -1$, and (b) $h_- = 1.1$.

5. IDENTIFICATION OF THE SEMILINEAR DUHEM MODEL

In this section we develop an identification method based on the semilinear Duhem model. Specifically, consider input-output curves $\hat{y}_+(u)$ and $\hat{y}_-(u)$, $u \in [u_{\min}, u_{\max}]$, that form a closed curve in $\mathbb{R}^2$. Then the semilinear Duhem model identification problem is to find an order n and matrices $A_+ \in \mathbb{R}^{n\times n}$, $A_- \in \mathbb{R}^{n\times n}$, $B_+ \in \mathbb{R}^n$, $B_- \in \mathbb{R}^n$, and $C \in \mathbb{R}^{1\times n}$ such that, $\hat{y}_+(u)$, $\hat{y}_-(u)$ satisfy (17), (18) in steady state with $E_+ = E_- = 0$ and $D = 0$. Furthermore, to guarantee convergence to the hysteresis map, we require that the stability condition $\rho(e^{\beta A_+}e^{-\beta A_-}) < 1$ be satisfied.

The semilinear Duhem model identification problem is equivalent to identifying two linear systems whose forward-time ramp response and backward-time ramp response coincide with $\hat{y}_+(u)$ and $\hat{y}_-(u)$, respectively under the stability condition. Note that the independent variable of the linear system (17) is nonmonotonic, since u is increasing for $\hat{y}_+(u)$ and decreasing for $\hat{y}_-(u)$. To avoid backward-in-time identification, we introduce a monotonically increasing independent variable, $\hat{u} \in [u_{\min}, 2u_{\max} - u_{\min}]$. Since the time-scale invariance property of the semilinear Duhem model renders the input-output map unaffected by the time dependence on u, we reparameterize $\hat{y}_+(u)$ and $\hat{y}_-(u)$ in terms of $\hat{u}$. Specifically, we 'flip over' $\hat{y}_-(u)$ as shown Figure 8 and define

$$\hat{y}(\hat{u}) \triangleq \begin{cases} \hat{y}_+(\hat{u}), & u_{\min} \le \hat{u} < u_{\max}, \\ \hat{y}_-(u_{\max} + u_{\min} - \hat{u}), & u_{\max} \le \hat{u} \le 2u_{\max} - u_{\min}, \end{cases}$$

$$u(\hat{u}) \triangleq \begin{cases} \hat{u}, & u_{\min} \le \hat{u} < u_{\max}, \\ \hat{u}_{\max} + u_{\min} - \hat{u}, & u_{\max} \le \hat{u} \le 2u_{\max} - u_{\min}. \end{cases}$$

Then the identification problem is to find system matrices associated with the input $\hat{u}(\hat{u})$ and the output $\hat{y}(\hat{u})$, $u \in [u_{\min}, 2u_{\max} - u_{\min}]$.

Now, let y_k and u_k, $k = 0, \ldots, 2l-1$, be $2l$ measurements taken from $\hat{y}(\hat{u})$ and $u(\hat{u})$, respectively. Then we determine system matrices $\hat{A}_+$, $\hat{A}_-$, $\hat{B}_+$, $\hat{B}_-$, and $\hat{C}$ to approximately satisfy the *discrete-time semilinear Duhem model*

$$x_{k+1} = \begin{cases} \hat{A}_+ x_k + \hat{B}_+ u_k, & k = 0, \ldots, l-1, \\ \hat{A}_- x_k + \hat{B}_- u_k, & k = l, \ldots, 2l-1, \end{cases} \quad (21)$$

$$y_k = \hat{C} x_k, \quad (22)$$

Note that the stability condition for (21), (22) is $\rho(A_+^l A_-^l) < 1$.

Finding system matrices is nontrivial, since the input u_k is not persistently exciting. Nevertheless, we use the nonminimal input/state/output representation approach. Suppose u_k and y_k satisfy the m-dimensional ARX model

$$\begin{aligned} y_{k+1} = {} & -\alpha_1^+ y_k - \cdots - \alpha_m^+ y_{k-m+1} \\ & + \beta_1^+ u_k + \cdots + \beta_m^+ u_{k-m+1}, \end{aligned} \quad (23)$$

for $k = 0, \ldots, l-1$, where $\alpha_i^+ \in \mathbb{R}$ and $\beta_i^+ \in \mathbb{R}$, $i = 1, \ldots, m$, are system parameters. Then (23)

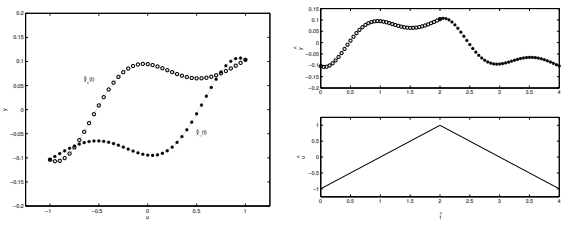

(a) (b)

Fig. 8. The given input-output curves $\hat{y}_+(u)$ and $\hat{y}_-(u)$ in (a) are considered as the input-output map of $\hat{y}(\hat{u})$ and $u(\hat{u})$ in (b).

has a nonminimal state space representation of order $2m-1^{\text{th}}$ given by

$$x_{k+1} = \hat{A}_+ x_k + \hat{B}_+ u_k, \quad k = 0, \ldots, l-1, \quad (24)$$

$$y_k = \hat{C} x_k, \quad (25)$$

where

$$x_k \triangleq \begin{bmatrix} y_k & \cdots & y_{k-m+1} & u_{k-1} & \cdots & u_{k-m+1} \end{bmatrix}^{\mathrm{T}},$$

$$\hat{A}_+ \triangleq \begin{bmatrix} -\alpha_1^+ & \cdots & -\alpha_{m-1}^+ & -\alpha_m^+ & \beta_2^+ & \cdots & \beta_{m-1}^+ & \beta_m^+ \\ 1 & \cdots & 0 & 0 & 0 & \cdots & \cdots & 0 \\ \vdots & \ddots & \vdots & \vdots & \vdots & & & \vdots \\ 0 & \cdots & 1 & 0 & 0 & \cdots & \cdots & 0 \\ 0 & \cdots & 0 & 0 & 0 & \cdots & 0 & 0 \\ 0 & \cdots & 0 & 0 & 1 & \cdots & 0 & 0 \\ \vdots & & \vdots & \vdots & \vdots & \ddots & \vdots & \vdots \\ 0 & \cdots & 0 & 0 & 0 & \cdots & 1 & 0 \end{bmatrix},$$

$$\hat{B}_+ \triangleq \begin{bmatrix} \beta_1^+ & 0 & \cdots & 0 \end{bmatrix}^{\mathrm{T}}, \quad \hat{C} \triangleq \begin{bmatrix} 1 & 0 & \cdots & 0 \end{bmatrix}.$$

We define $\hat{A}_- \in \mathbb{R}^{(2m-1)\times(2m-1)}$ and $\hat{B}_- \in \mathbb{R}^{2m-1}$ for $k = l, \ldots, 2l-1$ analogously. Note that the initial state x_0 for (24) involves data taken from the backward system of (21), namely, $y_{2l-1}, \ldots, y_{2l-m+1}$, and analogously for x_l. This ensures continuity of the state over $[u_{\min}, 2u_{\max} - u_{\min}]$.

Since x_k consists of inputs and outputs, we can immediately determine the state x_k for all $k = 0, \ldots, 2l-1$. Now, define $\Phi_{1_+} \in \mathbb{R}^{(2m-1)\times l}$, $\Phi_{2_+} \in \mathbb{R}^{(2m-1)\times l}$, and $U_{1_+} \in \mathbb{R}^{1\times l}$ as

$$\Phi_{1_+} \triangleq \begin{bmatrix} x_0 & x_1 & \cdots & x_{l-1} \end{bmatrix}, \; \Phi_{2_+} \triangleq \begin{bmatrix} x_1 & x_2 \cdots & x_l \end{bmatrix},$$

$$U_{1_+} \triangleq \begin{bmatrix} u_0 & u_1 & \cdots & u_{l-1} \end{bmatrix}.$$

Then $\hat{A}_+$, $\hat{B}_+$, $\hat{A}_-$ and $\hat{B}_-$ are determined from minimizing

$$\left\| \Phi_{2_+} - [\hat{A}_+ \; \hat{B}_+] \begin{bmatrix} \Phi_{1_+} \\ U_{1_+} \end{bmatrix} \right\|_{\mathrm{F}} + \left\| \Phi_{2_-} - [\hat{A}_- \; \hat{B}_-] \begin{bmatrix} \Phi_{1_-} \\ U_{1_-} \end{bmatrix} \right\|_{\mathrm{F}}, \quad (26)$$

subject to

$$\rho(A_+^l A_-^l) < 1. \quad (27)$$

Since the stability condition (27) is not convex, we use the fact that if $\bar{\sigma}(A) < 1$, where $\bar{\sigma}(A)$ is the maximum singular value of A, then $\rho(A) < 1$ and thus $\rho(A^l) < 1$. Then from the submultiplicative property of the maximum singular value, we have the alternative stability condition

$$\bar{\sigma}(A_+) < 1 \text{ and } \bar{\sigma}(A_-) < 1. \quad (28)$$

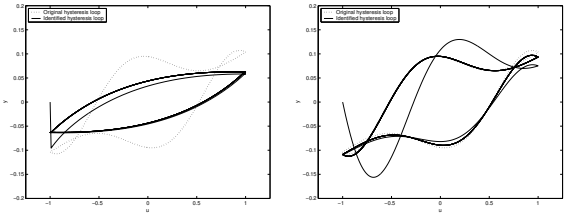

(a) (b)

Fig. 9. The identification of $\hat{y}_+(u)$, $\hat{y}_-(u)$ from Example 3 with (a) $p = 1$ and (b) $p = 7$.

Therefore, the original constrained least squares problem (26), (27) can be rewritten as two separate least squares problems with a convex constraint

$$\min_{A_+,B_+} \left\| \Phi_{2_+} - \begin{bmatrix} \hat{A}_+ & \hat{B}_+ \end{bmatrix} \begin{bmatrix} \Phi_{1_+} \\ U_{1_+} \end{bmatrix} \right\|_{\mathrm{F}}, \quad \text{subject to } \bar{\sigma}(A_+) < 1, \tag{29}$$

and

$$\min_{A_-,B_-} \left\| \Phi_{2_-} - \begin{bmatrix} \hat{A}_- & \hat{B}_- \end{bmatrix} \begin{bmatrix} \Phi_{1_-} \\ U_{1_-} \end{bmatrix} \right\|_{\mathrm{F}}, \quad \text{subject to } \bar{\sigma}(A_-) < 1. \tag{30}$$

The constrained least squares problems (29) and (30) are quadratic programming problem with positive-semi-definite constraints. Then we can find $\hat{A}_+$, $\hat{A}_-$, $\hat{B}_+$, and $\hat{B}_-$ by minimizing a linear function over symmetric cones. For details of a similar algorithm, see Lacy and Bernstein (2003).

Remark 1. The alternative stability condition (28) is conservative and may result an overly constrained solution. To avoid the conservatism, we consider $\bar{\sigma}(A_+) < p$ and $\bar{\sigma}(A_-) < p$, where $p \geq 1$. The condition $\rho(A_+^l A_-^l) < 1$ is checked a posteriori to verify stability.

Example 4. Suppose $\hat{y}_+(u)$ and $\hat{y}_-(u)$ are given as Figure 9 from Example 3. The identification is performed with $m = 2$, and thus the identified system is of order 3. Figure 9a shows the input-output map of the identified system with $p = 1$. Although $\rho(A_+^l A_-^l) = 0.0262$ and thus the stability condition is met, the least squares cost is 0.0553 and the input-output map poorly fits $\hat{y}_+(u)$ and $\hat{y}_-(u)$. Then the upper bound $p = 1$ is increased to $p = 7$, where $\rho(A_+^l A_-^l) = 0.0134$. The input-output map fits the original hysteresis better as shown in Figure 9b, and the least squares cost is 5.12×10^{-9}.

Example 5. Consider a dynamic stall model of an oscillating 2-D airfoil. The dashed line of Figure 10 represents dynamic stall between the angle of attack and the lift coefficient of an airplane (Carr *et al.*, 1977). The identification is performed with $m = 20$, hence the identified system is of order 39. Figure 10a shows the input-output map of the identified system and it does not fit the stall loop

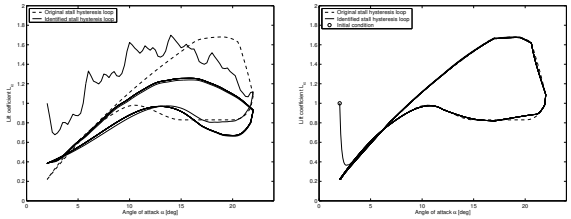

(a) (b)

Fig. 10. The identification of the dynamic stall model (a) without additional subintervals and (b) with 10 subintervals.

well. To improve the fit, we divide $[u_{\min}, u_{\max}]$ into 10 subintervals and identify the system matrices for each subintervals. Hence the model is a switching system which switches according to the subinterval of u. Figure 10b shows the input-output map of the identified system.

6. Conclusion

In this paper we introduced the rate-independent semilinear Duhem model. The analysis of this model was facilitated by a reparameterization in terms of the control input. By analyzing the iterated ramp response, we obtained sufficient conditions for convergence to a hysteresis map. Finally the semilinear Duhem model provided the basis for a least squares identification method based on a convex optimization algorithm.

REFERENCES

Campbell, S. L. and Jr. C. D. Meyer (1979). *Generalized Inverse of Linear Transformations*. Pitman Publishing Ltd.. London.

Carr, L. W., K. W. McAlister and W. J. McCroskey (1977). Analysis of the development of dynamic stall based on oscillating airfoil measurements. Technical Report TN D-8382. NASA.

Chua, L. O. and S. C. Bass (1972). A generalized hysteresis model. *IEEE Trans. Circuit Theory* **19**(1), 36–48.

Coleman, B. D. and M. L. Hodgdon (1986). A constitutive relation for rate-independent hysteresis in ferromagnetically soft materials. *Int. J. Eng. Sci.* **24**, 897–919.

Kransnosel'skii, M. A. and A. V. Pokrovskii (1980). *Systems with Hysteresis*. Springer-Verlag. New York, NY.

Lacy, S. S. and D. S. Bernstein (2003). Subspace identification with guaranteed stability using constained optimization. In: *Proc. Amer. Contr. Conf.* To be appeared.

Macki, J. W., P. Nistri and P. Zecca (1993). Mathematical models of hysteresis. *SIAM Review* **35**(1), 94–123.